GREEN TEA MEDIATED BIOSYNTHESIS OF α-Fe_2O_3 NANO-/ MICRO-PARTICLES AND THEIR CHARACTERIZATION

Bashir Ahmmad[*a], **Junichi Kurawaki**[b], **Takahiro Ohkubo**[a] **and Yasushige Kuroda**[a]

[a]Division of Chemistry and Biochemistry, Graduate School of Natural Science and Technology
Okayama University, 3-1-1 Tsushimanaka, Kita-ku, Okayama 700-8530, Japan
[b]Department of Chemistry and Bioscience, Graduate School of Science and Engineering
Kagoshima Universtiy, 1-21-35 Korimoto, Kagoshima 890-0065, Japan
*Corresponding author's e-mail: ahmmad-b@cc.okayama-u.ac.jp

Introduction

Iron oxide is one of the most frequently used catalysts in chemical industry, gas sensors materials, pigments, paint and also a potential candidate as a photoanode for possible photoelectrochemical cells [1-3].
Among various methods for the synthesis of nano or micro particles, hydrothermal synthesis process has some advantages, including mild synthetic conditions, simple manipulation and good crystallization of the products. However, hydrothermal synthesis often involves the usage of template, toxic or expensive chemicals and thus toxic byproducts immersing from these chemical reactions are often potentially dangerous to the environment. On the other hand, use of biological organisms such as microorganisms, plant extract or plant biomass could be an alternative to chemical and physical methods for the generation of metal or metal oxide nanoparticles in an eco-friendly manner[4]. To date, plant mediated synthesis is limited solely to metal nanoparitlces though bacteria assisted biosynthesis of metal oxides nanoparticles has been applied by some researchers [5]. To the best of our knowledge, here we report for the first time, the preparation of highly crystallized nanoparticles of mesoporous α-Fe_2O_3 by a simple hydrothermal method, using the extract of green tea leaves (*camellia sinensis*).

Experimental

Materials and method
Dry green tea leaves (2 g) were put into 150 ml water and heated at 80° C for 20 min on a hot plate. In a beaker 15 g of $Fe(NO_3)_3{\cdot}9H_2O$ or $FeCl_3{\cdot}6H_2O$ was dissolved in green tea and then the solution was transferred in a teflon lined autoclave and heated at 140° C for 13 h under ambient pressure. The autoclave was cooled to room temperature and the products were washed and dried. The as-prepared mesoporous nanoparticles were characterized by SEM, TEM, XRD, XPS, Raman, UV-visible spectroscopy, and nitrogen adsorption analysis. The photocatalytic activity of the nanoparticles was evaluated by the amount of hydroxyl radical formed under visible light irradiation detected by fluorescence spectroscopy. About 60 mg of the as-prepared α-Fe_2O_3 nanoparticles were added to 50 mL of 5×10^{-4} M terephthalic acid solution in 2×10^{-3} M NaOH, and then visible light irradiation to the solution was started. A xenon lamp (Ushio, 500 W) was used as a visible light source with an UV cut-off filter (L-42). For the measurement of the active oxidative species (mainly corresponding to hydroxyl radicals ($^{\bullet}OH$) produced by α-Fe_2O_3 nanoparticles), a fluorophotometer (Shimazu, RF-5300PC) was used. Sampling was performed in every 15 min.

Results and discussion

Characterization
The SEM images (Fig. 1a and b) of as-prepared α-Fe_2O_3 nano and microparticles demonstrate that the products consist of a nano or micro particles with uniform size and no aggregation is observed. As seen in the TEM images (Fig. 2a) the nanoparticles are somewhat spherical in shape with size ranges from 40 to 80 nm. Whereas the microparticles are somewhat elliptic shape (Fig. 2b) with diameter and length of 500 nm and 1μm, respectively. The selected-area electron diffraction (SAED) pattern in Fig. 2a (inset) reveals that the particles are polycrystalline nature. The average crystal size (t) was calculated using Scherer's equation, $t=0.89\lambda/\beta\cos\theta$, where, λ is the X-ray wavelength, β is the full width at half maximum of diffraction line and θ is the diffraction angle of the XRD spectra. The average crystal size was calculated to be 33 and 45 nm for as-prepared nano- and micro-particles, respectively.

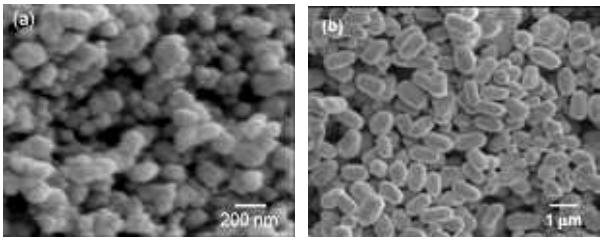

Fig. 1 SEM images of nano (a) and micro (b) particles of the as-prepared α-Fe_2O_3.

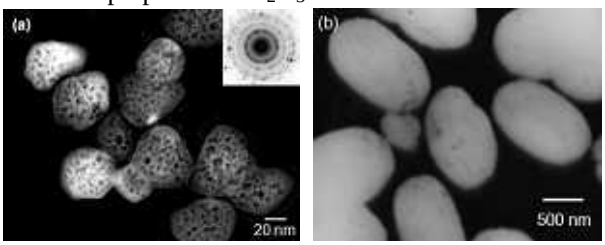

Fig. 2 TEM images of nano (a) and micro (b) particles of the as-prepared α-Fe_2O_3.

The XRD pattern of as-prepared nano and micro particles of α-Fe_2O_3 nanoparticles are shown in Fig. 3. For both nano and micro particles, the XRD peaks can be easily indexed to rhombohedral α-Fe_2O_3 with lattice parameters a= .5028 and c = 1.373 nm (Space Group: R3c), which are in agreement with the reported values (JCPDS 86-0550). No other peaks for impurities were observed.

The porosity of the as-synthesized α-Fe_2O_3 nano- and micro-particles were measured by the nitrogen adsorption-desorption isotherms and corresponding pore size distributions obtained by Barrett-Joyner-Halenda (BJH) method as shown in Fig. 4. The mesoporous hematite nanoparticles exibit a IV-type isotherm with H3-type hysteresis loop on the basis of the IUPAC classification [6]. IV-type isotherm is caused by the capillary condensation of mesopores and H3-type hysteresis loop is attributed to asymmetric slit-shape mesopores. The mesoporous hematite nanoparticles show broad pore size distribution at 3-15 nm with predominant pore diameter around at 4 and 7 nm. The surface area of as-prepared sample was found to be 19.8 m^2/g which is about 3 times higher than the commercial α-Fe_2O_3 (surface area of 7 m^2/g). The pore volume of the nanoparticles was found to be 0.036 cm^3/g. On the other hand negligible pores were found in microparticles and the BET surface area was found to be 5 m^2/g.

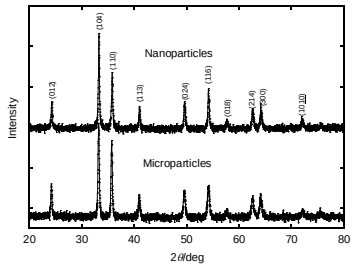

Fig. 3 XRD pattern of α-Fe_2O_3 nano and micro particles.

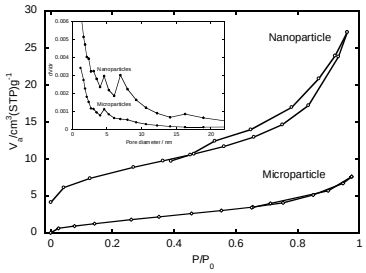

Fig. 4 Nitrogen adsorption isotherm of nano- and micro particles of α-Fe_2O_3 .

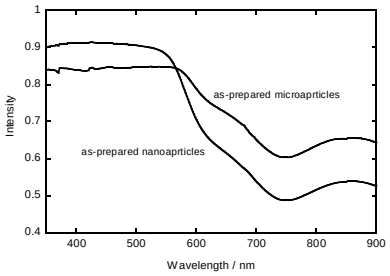

Fig. 5 UV-visible diffusion spectra for nano- and micro particles of α-Fe_2O_3 .

The UV-visible spectra of nano and microparticles of α-Fe_2O_3 are shown in Fig. 5. The absorption spectra exibit a broad absorption in the visible region, extending into the UV, with a tail extending to 570 nm. The optical absorption bands in visible and UV region are attributed to the transition in crystal field and the charge transfer processes and the difference in the absorbance is due to difference in their morphology and size.

Photocatalytic activity

Fig. 6 shows the plots of fluorescence intensity with as-prepared α-Fe_2O_3 nano-, micro-particles and commercial α-Fe_2O_3 nanoparticles after 1 h of visible light irradiation (λ > 400 nm). We can see that the as-prepared α-Fe_2O_3 nanoparticles show about two times higher activity than commercial α-Fe_2O_3 nanoparticles in terms of hydroxyl radical formation. The higher activity may emerge from the comparatively higher surface area and porosity in the as-prepared mesoporous α-Fe_2O_3 nanoparticles. However, the as-prepared microparticles show similar activity to commercial α-Fe_2O_3. The low activity can be attributed mainly to their low surface areas.

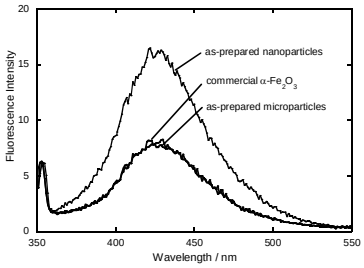

Fig. 6 Fluorescence spectra for as-prepared α-Fe_2O_3 nano-, micro-particles and commercial α-Fe_2O_3 nanoparticles.

Conclusion

We successfully prepared α-Fe_2O_3 nano- and micro-particles by a combination of hydrothermal and biosynthesis method. The method consisted of one-step synthesis process which gives highly crystallized mesoporous α-Fe_2O_3 nanoparticles. The as-prepared nanoparticles have about three times higher surface area compared to commercial α-Fe_2O_3 nanoparticles and two times higher activity in term of hydroxyl radical formed under visible light irradiation.

Acknowledgement

This work was partly supported by Grant-in-Aid for Scientific Research (No. 21020030). One of the authors (B.A.) acknowledges the financial support by the Sasakawa Scientific Research Grant from the Japan Science Society.

References

[1] P. Li, D. E. Miser, S. Rabiei, R. T. Yadav, M. R. Hajaligol, The removal of carbon monoxide by iron oxide nanoparticles, *Appl. Catal. B: Environ.* 43 (2003) 151-162.
[2] J. Chen, L. Xu, W. Li, X. Gou, α-Fe_2O_3 Nanotubes in Gas Sensor and Lithium-ion Battery Applications, *Adv. Mater.* 17 (2005) 582-586.
[3] T. Lindgren, H. Wang, N. Beermann, L. Vayssieres, A. Hagfeldt, S.-E. Lindquist, Aqueous photoelectrochemistry of hematite nanorod array, *Sol. Energ. Mat. Sol. C.* 71 (2002) 231-243.
[4] K. Leonard, B. Ahmmad, H. Okamura, J. Kurawaki, In situ green synthesis of biocompatible ginseng capped gold nanoparticles with remarkable stability, *Colloid. Surfac. B*, 82 (2011) 391-396.
[5] P. Mohanpuria, N. K. Rana, S. K. Yadav, Biosynthesis of nanoparticles: technological concepts and future applications, *J Nanopart. Res.* 10 (2008) 507-517
[6] K. S. W. Sing, D. H. Everett, R. A. W. Haul, L. Moscou, R. A. Pierotti, J. Rouquerol, T. Siemieniewska Reporting Physisorption Data for Gas/Solid Systems, *Pure Appl. Chem.* 57 (1985) 603-619.